

The Golgi Comprises a Paired Stack that Is Separated at G2 by Modulation of the Actin Cytoskeleton through Abi and Scar/WAVE

Vangelis Kondylis,¹ Hezder E. van Nispen tot Pannerden,^{1,2} Bram Herpers,¹ Florence Friggi-Grelin,³ and Catherine Rabouille^{1,*}

¹The Cell Microscopy Centre, Department of Cell Biology, Institute of Biomembranes, University Medical Centre Utrecht, Heidelberglaan 100, 3584 CX Utrecht, The Netherlands

²Department of Molecular Cell Biology, Institute of Biomembranes, Utrecht University, 3584 CH Utrecht, The Netherlands

³Institut de Recherches Signalisation, Biologie du Développement et Cancer, CNRS UMR 6543, Centre de Biochimie, Parc Valrose, 06108 Nice cedex 2, France

*Correspondence: c.rabouille@umcutrecht.nl

DOI 10.1016/j.devcel.2007.03.008

SUMMARY

During the cell cycle, the Golgi, like other organelles, has to be duplicated in mass and number to ensure its correct segregation between the two daughter cells. It remains unclear, however, when and how this occurs. Here we show that in *Drosophila* S2 cells, the Golgi likely duplicates in mass to form a paired structure during G1/S phase and remains so until G2 when the two stacks separate, ready for entry into mitosis. We show that pairing requires an intact actin cytoskeleton which in turn depends on Abi/Scar but not WASP. This actin-dependent pairing is not limited to flies but also occurs in mammalian cells. We further show that preventing the Golgi stack separation at G2 blocks entry into mitosis, suggesting that this paired organization is part of the mitotic checkpoint, similar to what has been proposed in mammalian cells.

INTRODUCTION

During the cell cycle, the Golgi, like other organelles, has to duplicate in mass and/or number to ensure its correct segregation between the two daughter cells. It remains unclear, however, when and how this occurs.

The process of Golgi duplication and inheritance in mammalian cells is still debated, as different modes of Golgi biogenesis have been proposed (Shorter and Warren, 2002; Bevis et al., 2002; Pecot and Malhotra, 2004; Altan-Bonnet et al., 2006). One reason why this issue is not yet settled could be due to the elaborate organization of the Golgi stacks, which are interconnected to form a single-copy organelle capping the nucleus, thus impeding clear visualization of organelle duplication and segregation. Therefore, we have exploited the relatively small number of Golgi stacks in *Drosophila* tissue-cultured S2 cells to revisit this issue.

In S2 cells, the Golgi stacks are found in close proximity to transitional endoplasmic reticulum (tER) sites, forming tER-Golgi units (Kondylis and Rabouille, 2003; Herpers and Rabouille, 2004). We observed that their number nearly doubles at G2 phase (see Results). In an effort to identify factors mediating this process, we focused on cytoskeletal elements that have been involved in the organization of the mammalian Golgi apparatus. Microtubules are involved in mammalian Golgi ribbon maintenance, as their depolymerization leads to its reorganization into individual Golgi stacks in close proximity to ER exit sites (Thyberg and Moskalewski, 1999; Hammond and Glick, 2000).

F-actin has also been implicated in the organization of the mammalian Golgi apparatus, as its depolymerization leads to a compact appearance of this organelle without disruption of cisternal stacking (De Matteis and Morrow, 2000; Egea et al., 2006; and references therein). A key regulator of actin polymerization is the Arp2/3 complex. Its F-actin nucleation activity is triggered both by Wiskott-Aldrich syndrome protein (WASP) and WASP family verprolin-homologous (WAVE/Scar) proteins (Stradal et al., 2004), which are in turn regulated by Rho small GTPases. WASP exists in an autoinhibited state that is released by the cooperative action of Cdc42, PI(4,5)P, and other SH3-containing proteins (Stradal et al., 2004; and references therein). On the other hand, WAVE/Scar proteins, together with Sra-1, Kette (Nap1), Abi, and HSPC300, form a stable complex, which is itself regulated by Rac (Stradal et al., 2004; and references therein).

Rho GTPases have recently been implicated in maintaining Golgi architecture. Cdc42 has been localized on the Golgi membrane (Matas et al., 2004) and shown to recruit the Arp2/3 complex around this organelle via ARHGAP10 (Dubois et al., 2005). Furthermore, suppression of the brain-specific Rho-binding protein Citron-N in neurons was shown to lead to fragmentation of the Golgi apparatus, and Rho1 was proposed to exert its local effect on F-actin by regulating ROCK and profilin activity (Camera et al., 2003).

Here we show that drug-induced F-actin depolymerization in S2 cells leads to doubling of the number of

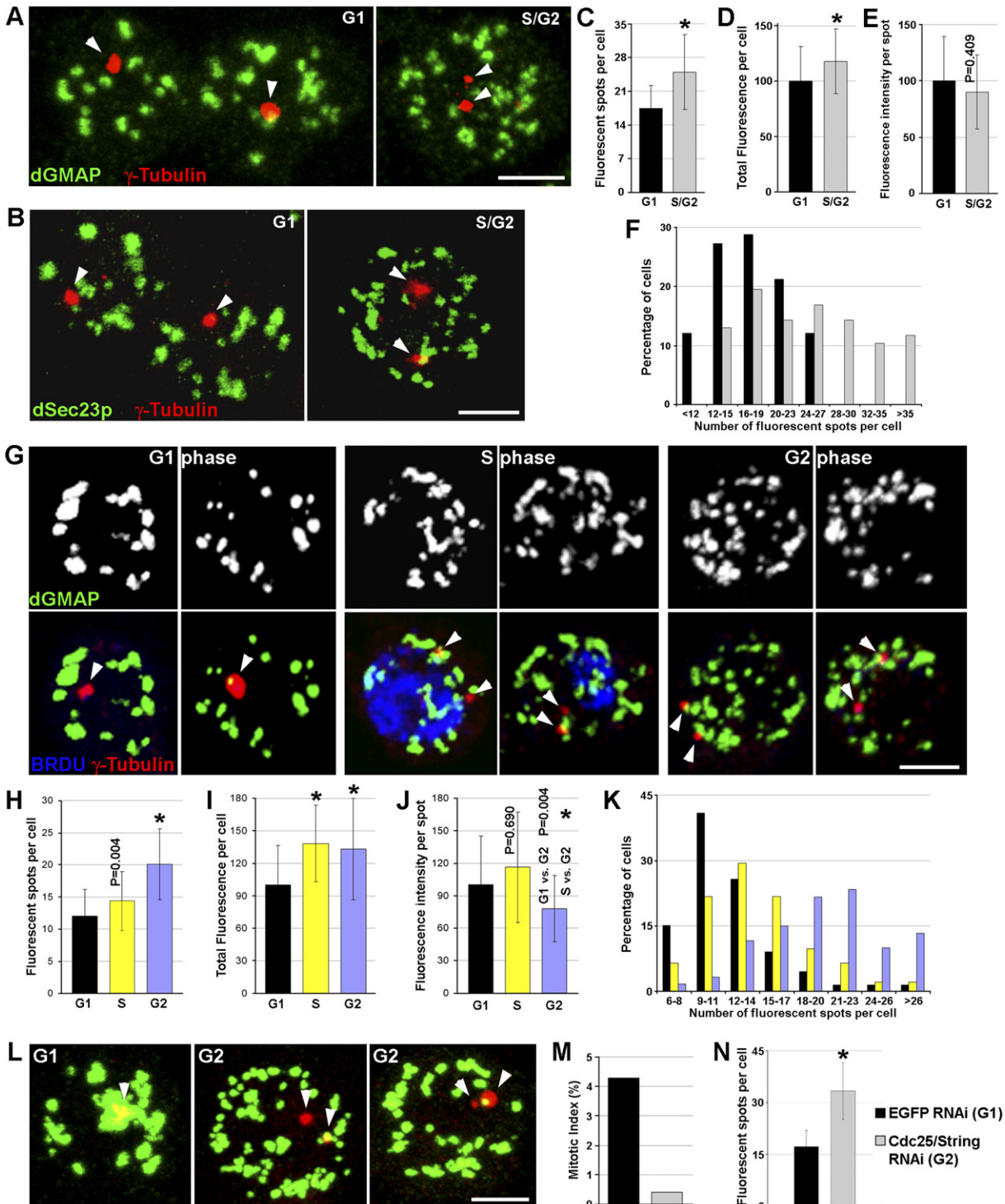


Figure 1. In *Drosophila* S2 Cells, tER-Golgi Units Separate at G2 Phase

(A and B) Immunofluorescence (IF) visualization of the Golgi (dGMAP, [A]) and tER sites (dSec23p, [B]) in S2 cells in G1 phase (one centrosome marked by γ -tubulin) and S/G2 phase (two centrosomes in close proximity).

(C–F) ImageJ quantification of the number of fluorescent Golgi spots per cell at G1 and S/G2 (C), the total fluorescence per cell (D), and the average fluorescence intensity per spot (E). Histogram showing the spread of the number of fluorescent spots per cell at G1 and S/G2 (F). Note that the number of spots increases at S/G2.

(G) IF visualization of the Golgi and the centrosome(s) in S2 cells where BrdU has been incorporated to mark cells in S phase (two centrosomes). Cells in G1 and G2 have no BrdU and one and two centrosomes, respectively.

tER-Golgi units independent of anterograde transport. Using live cell imaging, electron microscopy, and three-dimensional (3D) electron tomography, we show that each Golgi is organized as a pair of stacks held together by an actin-based mechanism, both in *Drosophila* and in human cells. In S2 cells, this is mediated by Abi and Scar, suggesting a novel role for the Rac signaling cascade in Golgi architecture. Last, we show that the Golgi stacks undergo separation at G2 through modulation of Abi and Scar, and that blocking this separation prevents cells from entering mitosis, supporting the existence of a G2/M checkpoint related to Golgi structural organization.

RESULTS

The Number of tER-Golgi Units Doubles at G2

In a nonsynchronized population of *Drosophila* S2 cells, the average number of tER-Golgi units per cell is relatively constant (Kondylis and Rabouille, 2003; Kondylis et al., 2005). However, it is apparent that larger cells, presumably at G2 phase, exhibit more. Using γ -tubulin (Savvidou et al., 2005) and centrin (Sanders and Salisbury, 1994) to mark the centrosome(s), we found that cells at S/G2 (two centrosomes in close proximity) exhibit ~ 25 tER-Golgi units, a 1.45-fold increase when compared to G1 cells (~ 17 ; Figures 1A–1C and 1F; see Table S1 in the Supplemental Data available with this article online).

To mark cells in S phase and distinguish them from G2, we performed a short bromodeoxyuridine (BrdU) incorporation (Figure 1G). Although the procedure for BrdU labeling leads to a reduction in the number of Golgi spots, the G2 cells (two centrosomes, BrdU-negative) exhibited on average 1.7-fold more Golgi spots than G1 cells (one centrosome, BrdU-negative), whereas the number of spots between G1 and S phase only increased marginally (Figures 1H and 1K; Table S1), indicating that a tER-Golgi near-doubling takes place at G2.

To confirm these results, we used RNAi to deplete String/Cdc25, which is known to result in a G2/M arrest in S2 cells (Moshkin et al., 2007). Indeed, upon 3 day depletion, the mitotic index dropped sharply (Figure 1M), and 90% of the cells were larger and exhibited two centrosomes (Figure 1L) due to their arrest in G2. Cdc25/String-depleted cells exhibited a 1.95-fold increase in the number of tER-Golgi units when compared to the G1 in mock-depleted cells (Figure 1N; Table S1).

In principle, the near-doubling in Golgi number at G2 could originate from the splitting of old Golgi or from their de novo formation (Munro, 2002). The latter scenario would predict an increase both in the total fluorescence

per cell and the number of Golgi spots. However, although the total fluorescence increases reproducibly by 40% between G1 and S cells (Figure 1I), it is not accompanied by an equivalent increase in the number of Golgi spots (Figure 1H). It is only during the S-to-G2 transition that the number of spots nearly doubles, together with a 33% decrease in the fluorescence intensity per spot (Figure 1J). This suggests that the Golgi grows/duplicates in mass during G1 and S phases, followed by its separation/scission at G2 (see below).

Upon entry of S2 cells into mitosis, tER sites (Figure S1A, prophase-metaphase) and Golgi stacks (Stanley et al., 1997; Figure S1B) disassemble. In late anaphase, tER-Golgi units are gradually rebuilt and the daughter cells inherit about half of them (Figure S1, anaphase-cytokinesis), in a fashion similar to mammalian ER exit sites (Stephens, 2003) and Golgi (Shima et al., 1997).

These results show that S2 cells double the number of their tER-Golgi units at G2 before their fragmentation and partitioning during mitosis.

F-Actin Depolymerization Also Leads to the Doubling of tER-Golgi Units

To investigate the molecular mechanism involved in the increase in the number of tER-Golgi units observed at G2, we tested drugs that affect microtubule and F-actin dynamics. In S2 cells, microtubule depolymerizing drugs do not alter tER-Golgi unit organization (Figure S2) or anterograde transport from the ER to the plasma membrane (PM; data not shown). In contrast, F-actin depolymerization by cytochalasin D (CytoD) or latrunculin B (LatB) (Figure S3A) led to a 1.7-fold increase in the number of fluorescent tER-Golgi spots (Figures 2A and 2B). The effect was complete after ~ 30 min (data not shown). All Golgi and tER markers examined exhibited the same behavior (Figure S3B). This effect was reversible upon LatB washout (data not shown).

F-actin depolymerization also led to similar doubling of the tER-Golgi units in S2R⁺ cells, a variant of S2 cells that are flatter and more adherent, and other *Drosophila* tissues (Figures S3C and S3D). Furthermore, the treatment did not lead to Golgi stack vesiculation (see below).

Using a previously established assay that measures the transport efficiency of the transmembrane protein Delta from the ER to PM (Kondylis and Rabouille, 2003; Kondylis et al., 2005), we found that after F-actin depolymerization, S2 cells were still anterograde transport competent (Figure 2E), similar to mammalian cells (Valderrama et al., 2001). However, Delta endocytosis was largely inhibited (Figure 2E), in line with the proposed role of

(H–K) ImageJ quantification of the same parameters as in (C)–(F) for S2 cells in G1, S, and G2 phase. Note that these numbers are smaller than in non-BrdU-incorporated cells, probably because the BrdU staining procedure compromised the immunofluorescence. However, the number of spots increases between G1 and G2 cells by 1.6-fold (see Table S1). In (J), the change in fluorescence intensity per spot in G2 cells is compared to that in both G1 and S cells. The p value for this latter comparison is significant.

(L–N) IF visualization of the Golgi and the centrosome(s) in S2 cells depleted of Cdc25/String by RNAi that accumulate at G2 (L) and display a doubling in their number of Golgi spots (quantified by ImageJ) (N). The mitotic index is reduced by 95% (M).

Arrowheads point to centrosome(s). Error bars represent standard deviation (SD), and asterisks indicate conditions under which a statistical significant change ($p \leq 0.001$) is calculated. This is always in reference to G1 mock-treated or mock-depleted cells, except Figure 1J (see above). The scale bars represent 5 μ m.

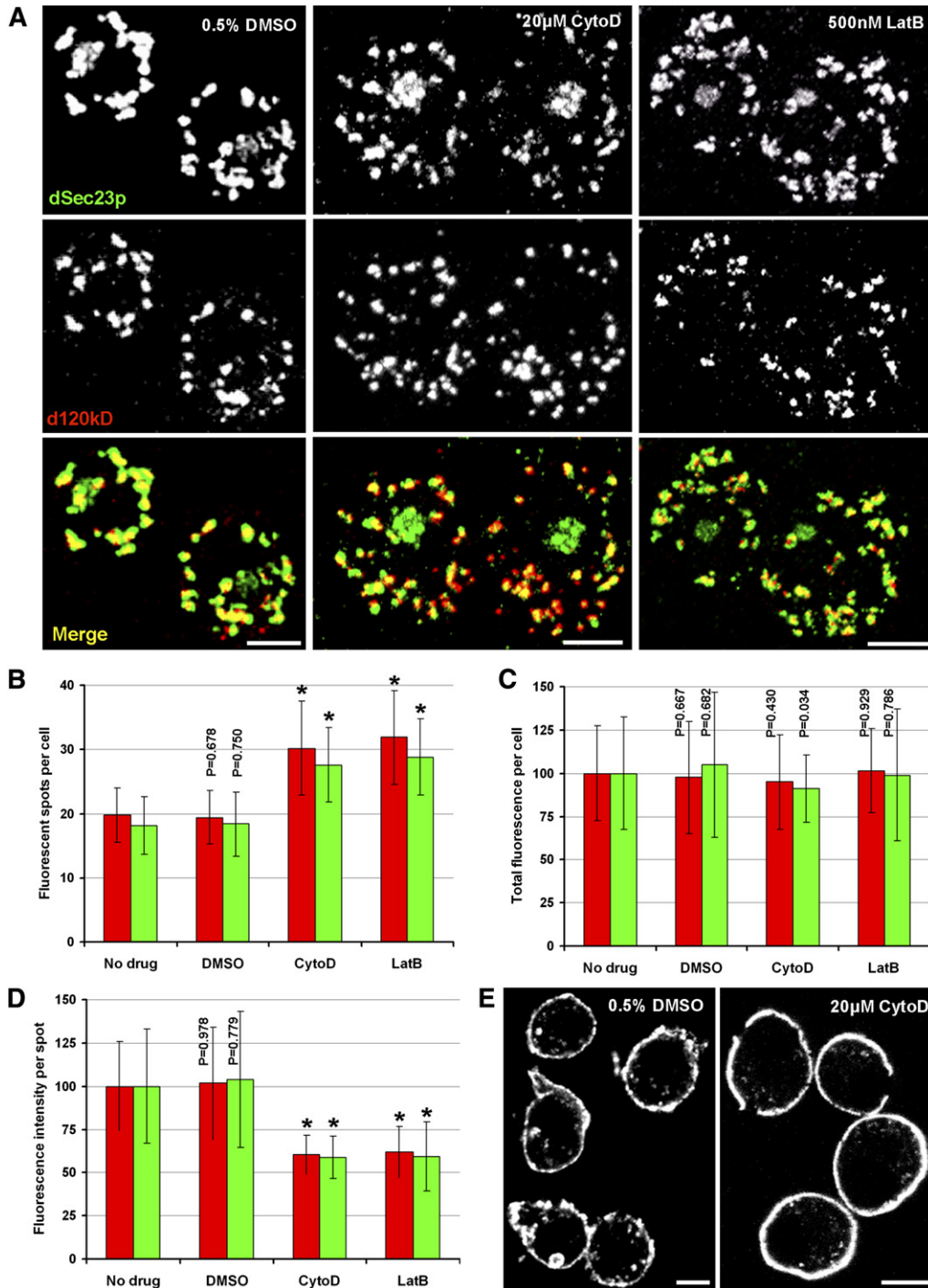


Figure 2. F-Actin Depolymerization in *Drosophila* S2 Cells Leads to a Doubling in the Number of tER-Golgi Units

(A) IF visualization of the Golgi (d120kD, red) and tER sites (dSec23p, green) in S2 cells treated with F-actin depolymerizing drugs. Note the increased number of fluorescent spots corresponding to tER-Golgi units.

(B–D) ImageJ quantification of the number of fluorescent objects per cell (B), the total fluorescence per cell (C), and the average fluorescence intensity per spot (D). Color coding as in (A). Error bars represent standard deviation (SD), and asterisks indicate conditions under which a statistical significant change ($p \leq 0.001$) is calculated.

(E) IF localization of Delta to estimate the efficiency of its anterograde transport to the plasma membrane in mock- and CytoD-treated Delta S2 cells. The scale bars represent 5 µm.

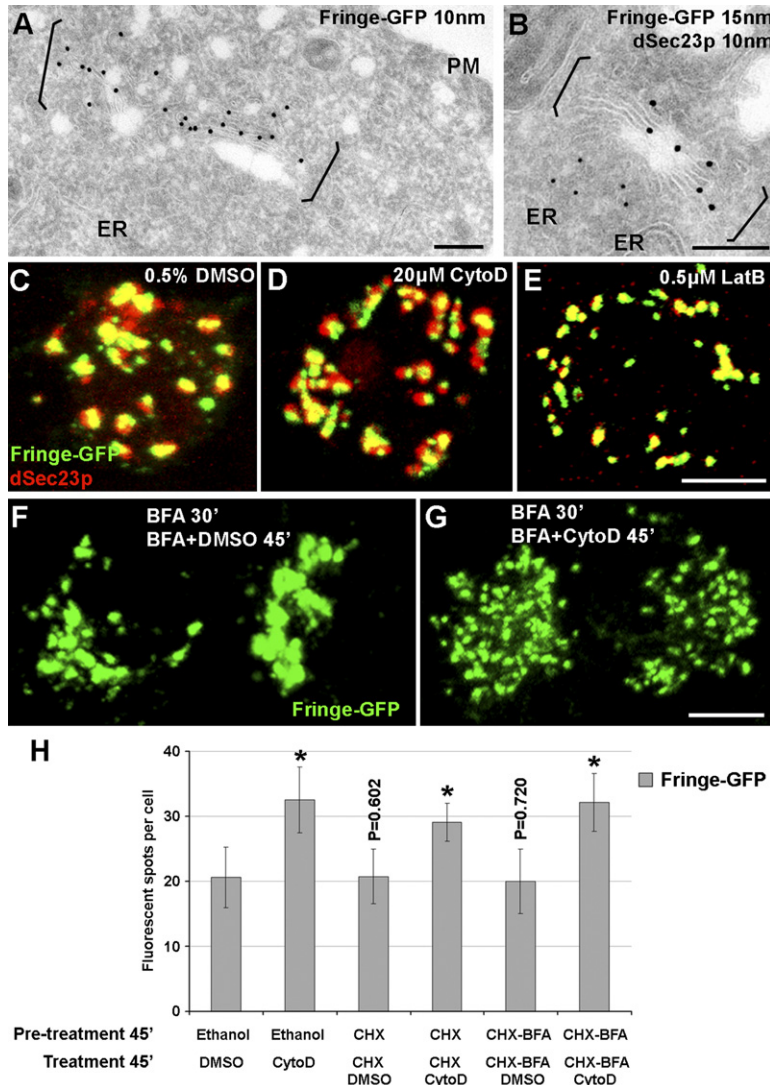


Figure 3. The New Golgi Originates from a Preexisting Golgi Membrane in an Anterograde Transport-Independent Fashion

(A and B) Localization by immunoelectron microscopy (IEM) of Fringe-GFP in transiently transfected S2 cells. Note the exclusive localization of Fringe-GFP on Golgi stacks (between brackets) and its clear segregation from the closely associated tER sites in (B). ER, endoplasmic reticulum; PM, plasma membrane.

(C–E) Visualization of Fringe-GFP and tER sites (dSec23p) upon F-actin depolymerization.

(F and G) Visualization of Fringe-GFP in S2 cells incubated with BFA to inhibit ER-Golgi transport followed by F-actin depolymerizing drugs. (H) Manual quantification of F-actin depolymerization effects upon inhibition of ER-Golgi transport and Fringe-GFP synthesis. Error bars represent standard deviation (SD), and asterisks indicate conditions under which a statistical significant change ($p \leq 0.001$) is calculated.

The scale bars in (A) and (B) represent 200 nm and in (C)–(G), 5 μ m.

the actin cytoskeleton in several endocytic pathways (Engqvist-Goldstein and Drubin, 2003).

The Golgi Is Split into Two upon F-Actin Depolymerization

As in G2 cells, the near-doubling in the number of tER-Golgi units upon F-actin depolymerization could be explained by the scission of the tER-Golgi units present before drug treatment, or could rely on their de novo formation (Munro, 2002). ImageJ quantification showed that the total fluorescence remains constant under all conditions (Figure 2C), whereas the average fluorescence intensity per Golgi or tER spot decreased by 40% (Figure 2D), suggesting that tER-Golgi units are split into two.

To test this hypothesis further, we followed the Golgi fate upon F-actin depolymerization using S2 cells expressing the green fluorescent protein (GFP)-tagged transmembrane Golgi O-linked N-acetyl-glucosaminyl-transferase Fringe (Munro and Freeman, 2000). Fringe-GFP was expressed in such a way that it marked exclu-

sively the Golgi stack membrane and is not present as a newly synthesized pool in the ER (see [Experimental Procedures](#); [Figures 3A](#) and [3B](#)). Our reasoning was that if the preexisting Golgi split, they would supply the membrane for the newly formed ones. Conversely, if new Golgi are formed de novo, the contribution of the old Golgi membrane would be marginal. Treatment with CytoD or LatB resulted in a near-doubling of Fringe-positive spots that remained closely associated with dSec23p that also doubled ([Figures 3C–3E](#) and [3H](#)). This indicates that the newly formed Golgi derive from scission of the pre-existing ones.

As anterograde transport is not inhibited by F-actin depolymerization ([Figure 2E](#)), it could also contribute to Golgi doubling. To test this, we analyzed the tER-Golgi number in Fringe-GFP-expressing cells treated with brefeldin A (BFA), which blocks ER-Golgi transport very efficiently (Kondylis and Rabouille, 2003). However, contrary to mammalian cells, where BFA induces redistribution of the Golgi membrane to the ER (Lippincott-Schwartz

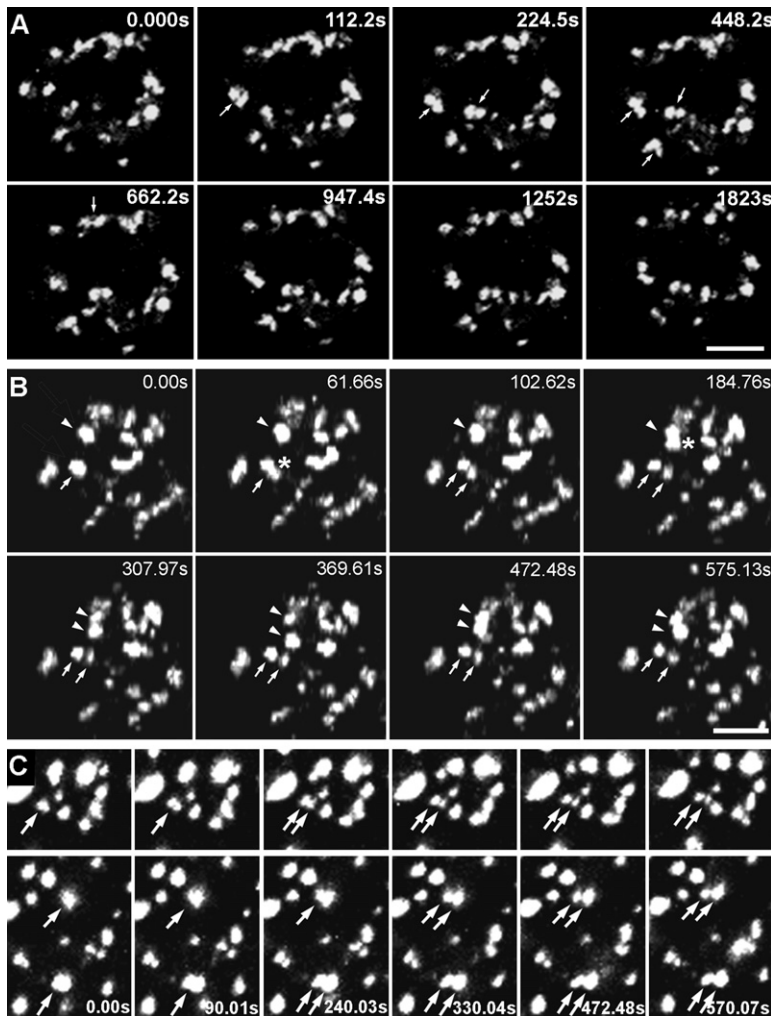


Figure 4. Golgi Stacks Undergo Scission upon F-Actin Depolymerization

(A and B) Selected images from time-lapse movies of Fringe-GFP-expressing S2 cells treated with DMSO (A) or CytoD (B). Each image represents a projection of five and seven confocal sections spanning a 1.7 μm and 3.2 μm part of the cell, respectively. The arrows in (A) point to transient Fringe-GFP-positive membrane connections between neighboring Golgi during the 30 min imaging. The arrows and arrowheads in (B) point to fluorescent spots that split during the 10 min imaging and the asterisks indicate the first appearance of a bilobed Golgi structure.

(C) Selected images from a movie of a GalNAcT2-GFP expressing HeLa cell treated with nocodazole and LatB. Each image represents a projection of five confocal sections spanning 1.7 μm of two different areas of a cell. Arrows indicate three spots undergoing fission. All fission profiles in (B) and (C) were verified by tracking the spots on single confocal sections. The complete movies are presented in [Supplemental Data](#).

The scale bars represent 5 μm .

et al., 1989), in S2 cells, the Golgi stacks remain largely intact (Figure S4A), although they often tend to cluster on one side of the nucleus (Figure 3F; Figure S4B; Kondylis et al., 2005).

F-actin depolymerization of BFA-treated S2 cells led to tER-Golgi near-doubling in a manner indistinguishable from untreated cells, irrespective of whether Fringe-GFP or endogenous Golgi and tER site markers were examined (Figures 3F–3H; Figures S4C and S4D). This indicates that tER-Golgi scission upon F-actin depolymerization is independent of ER-Golgi transport.

Live Cell Imaging of Golgi Scission

Our results suggest that upon F-actin depolymerization, each Golgi splits in two. To test this, we followed Golgi stacks using time-lapse confocal microscopy on Fringe-GFP S2 cells. In nontreated cells, the Golgi stacks exhibit only restricted movement (Figure 4A; Movie S1), as has been reported in other animal cells with equivalent tER-Golgi organization (Storrie et al., 1998; Bevis et al., 2002; Stephens, 2003). Occasionally, neighboring Golgi stacks were observed to associate transiently or ex-

change Fringe-GFP-positive membrane (arrows in Figure 4A; Movie S1).

When cells were filmed after 10 min incubation with CytoD or LatB, we observed Fringe-GFP-labeled Golgi spots undergoing scission generating two spots of roughly half the size of the original one. The scission events were not synchronous for all the spots in the same cell. It takes, on average, 105 ± 52 s ($n = 35$) to generate two distinct Golgi spots from a single one, starting with the formation of a bilobed profile (Figure 4B, asterisks). We never observed more than one Golgi scission event per Golgi spot, at least within the time frame of each movie.

The two fluorescent spots could either remain separated (arrows in Figure 4B and Movie S2) or appear to reunify and separate again (arrowheads in Figure 4B and Movie S2). This seems likely to reflect the movement of the two recently separated fluorescent spots toward each other reaching a distance below the resolution of light microscopy. This could explain why in fixed treated cells the number of tER-Golgi spots is increased by a factor lower than 2. Although not tested by live cell imaging, the results obtained with fixed cells suggest that the tER sites also undergo similar scission.

Mammalian Golgi Also Undergoes Scission

So far, the depolymerization of F-actin in mammalian cells has not permitted the visualization of Golgi scission similar to that we observed in S2 cells. This may be due to the structural complexity of the mammalian Golgi apparatus or additional functions of the actin cytoskeleton in these cells, such as the maintenance of intra-Golgi pH (Lazaro-Diequez et al., 2006).

Our previous studies have pointed out that the exocytic pathway of *Drosophila* cells resembles in many respects that of mammalian cells, in which microtubules are depolymerized (Kondylis and Rabouille, 2003; Kondylis et al., 2005). To induce an “S2 cell-like” tER-Golgi organization and assess Golgi scission upon F-actin depolymerization, GalNAcT2-GFP HeLa cells (stably expressing the Golgi resident enzyme N-acetyl-galactosaminyltransferase2 tagged with GFP; Storrie et al., 1998) were pretreated with nocodazole followed by addition of LatB, and filmed by time-lapse confocal microscopy. Analysis of such movies showed that several Golgi stacks per cell underwent scission during the 10 min of filming (arrows in Figure 4C and Movie S3) with similar characteristics but slower kinetics than in S2 cells (189 ± 100 s versus 105 ± 52) ($n = 33$). Golgi scission was not observed in cells treated only with nocodazole.

In agreement with an earlier study that reported an increase in the number of mammalian Golgi stacks parallel to a decrease in their size (Polishchuk et al., 1999), our results show that Golgi stacks in mammalian cells, as in S2 cells and other *Drosophila* tissues, also undergo scission upon F-actin depolymerization. This suggests that the Golgi consists of a duplicated structural unit.

The Golgi Comprises a Paired Stack

This duplicated structural unit could correspond to two structural preexisting entities that are maintained very close together, or to one morphologically uniform structure with an underlying yet unknown molecular discontinuity/asymmetry. Upon examination of electron microscopy (EM) sections of S2 cells, we identified many Golgi profiles showing two stacks close together forming a pair (Figure 5D). A pair is defined by the rim of one cisterna in one stack being less than 70 nm away from the rim of the closest cisterna in the second stack (Figures 5A and 5B; Figures S5A and S5B).

To test whether the typical organization of the Golgi is paired stacks, we performed 3D electron tomography on 250–500 nm thick sections and subsequent organelle modeling. These 3D reconstructions beautifully illustrate the proposed paired Golgi stack organization (Figures 5H–5K; Movies S4 and S5). Thus far, no clear tubular connections between equivalent cisternae of the paired stacks have been observed, but interestingly, in one tomogram, a pair of stacks shares a tubular network at its *cis* side (Figure 5I; Movie S5).

Upon F-actin depolymerization, although the total number of stacks is not significantly changed compared to mock-treated cells (Figure 5E), the occurrence of paired stacks is reduced by 60% (Figure 5D). Instead, individual

stacks are observed (Figure 5C; Figure S5C) whose average cross-sectional cisternal diameter is comparable to that of nontreated cells (320 ± 46 nm for LatB- and 305 ± 53 nm for CytoD-treated cells versus 308 ± 37 nm in DMSO-treated cells). Furthermore, mirroring our immunofluorescence data analysis, the total surface density of the tER-Golgi units is similar under all conditions (Figure 5F), but the surface density of individual units is reduced by ~50% (Figure 5G). These results indicate that the paired tER-Golgi units undergo separation into individual units upon F-actin depolymerization, suggesting that their pairing is F-actin mediated.

Abi and Scar/WAVE Maintain the Integrity of Paired Golgi Stacks

The dynamics of the actin cytoskeleton at the plasma membrane, but also around the mammalian Golgi apparatus, is regulated by Rho GTPases (Jaffe and Hall, 2005; Camera et al., 2003; Dubois et al., 2005; see Introduction). To investigate whether any of these GTPases are involved in the actin-based mechanism joining the paired Golgi stacks, we first overexpressed known dominant-negative forms of Cdc42, Rac1, and Rho1 (Feig, 1999). Expression of Cdc42^{T17N} and Rac^{T17N} led to tER-Golgi near-doubling (Figures S6B and S6C) compared to nonexpressing cells (Figure S6A). In contrast, Rho1^{T19N} overexpression did not alter the number of Golgi stacks (Figure S6D). These results indicated that Rac1 and/or Cdc42, but not Rho1, could regulate the pairing of the two Golgi stacks.

To test this further, we depleted specific downstream effectors of these GTPases. Cdc42 and Rac1 are known to promote microfilament branching by activating the actin-nucleating Arp2/3 complex, through WASP and Scar/WAVE, respectively. The latter forms a pentameric complex comprising Abi, among other proteins (see Introduction). Therefore, Scar, Abi, and WASP were depleted by RNAi (Figure 6). As previously reported, depletion of Abi leads to Scar degradation (data not shown; Kunda et al., 2003). We also found that Scar depletion leads to Abi depletion (Figure 6A), suggesting that Scar itself regulates the integrity of the pentameric complex. In contrast, WASP remains unaffected upon Abi or Scar RNAi, and the converse is also true (Figure 6A).

Similar to the F-actin depolymerization phenotype, Scar and Abi depletion led to a near-doubling (~1.7-fold increase) in the number of Golgi (Figures 6C, 6D, and 6F; Table S1) and tER sites (data not shown) in 90% of cells, concomitant with a ~35% decrease in fluorescent object size (Figure 6H). Accordingly, the majority of depleted cells exhibited a significant F-actin disruption (compare phalloidin staining in Figure 6B and Figures 6C and 6D). Conversely, WASP-depleted cells did not exhibit significant changes in the number or apparent morphology of their tER-Golgi units (Figures 6E–6H).

Taken together, these results suggest that the F-actin-dependent maintenance of paired Golgi stack organization is mediated by the Scar/Abi complex, possibly through Rac, but not Cdc42/WASP. Strengthening this result, actin (Figure S5D), endogenous Scar (Figure 7A),

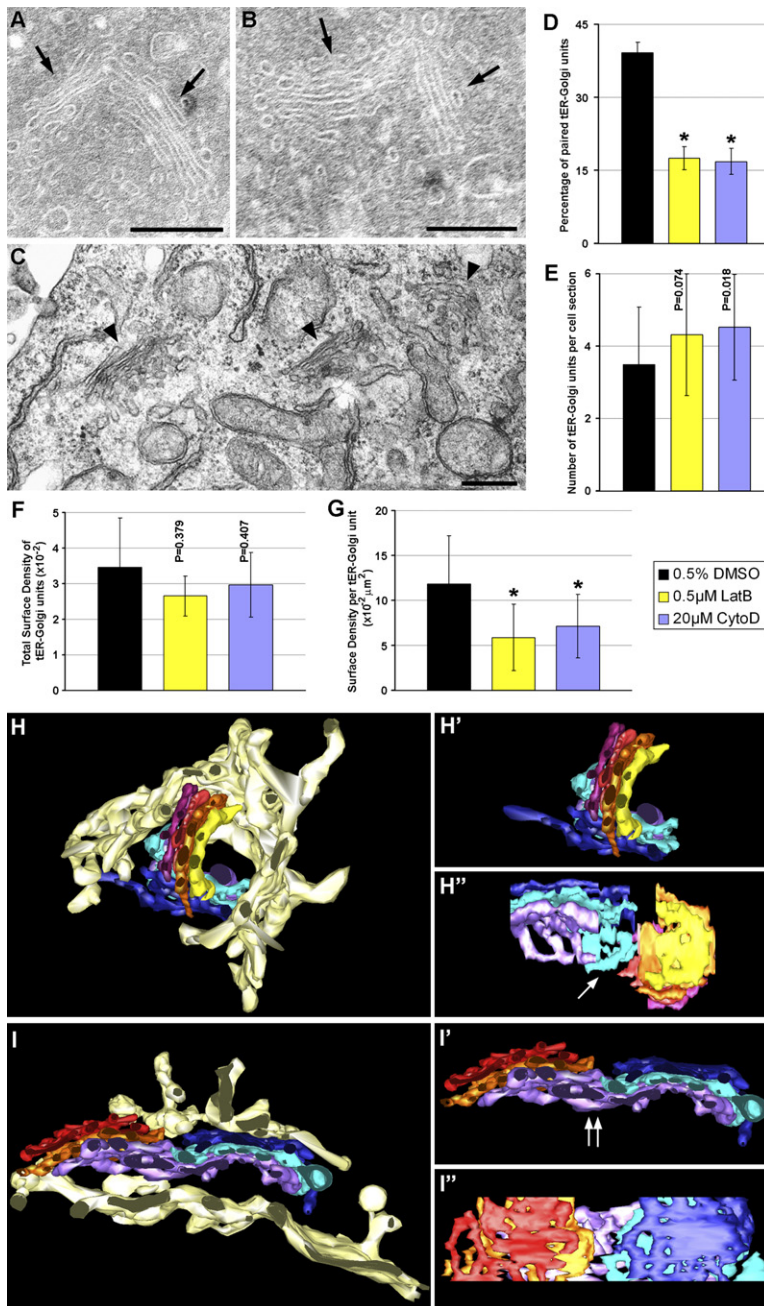


Figure 5. The Golgi Comprises a Paired Stack

(A and B) EM profiles of paired Golgi stacks (arrows) in cryosections of DMSO-treated S2 cells.

(C) EM profiles of individual Golgi stacks in sections of LatB-treated S2 cells (500 nM, 30 min). See more examples in Figures S5A–S5C.

(D–G) Stereological analysis of tER-Golgi unit ultrastructural organization upon F-actin depolymerization. Frequency of paired Golgi stacks among all Golgi profiles in mock-, CytoD-, and LatB-treated cells (D). Number of tER-Golgi units per cell section; a paired one was counted as two (E). Total surface density of tER-Golgi units (F). Surface density per individual tER-Golgi unit (G). Error bars represent standard deviation (SD), and asterisks indicate conditions under which a statistical significant change ($p \leq 0.001$) is calculated.

(H–I'') Three-dimensional reconstructions by electron tomography of two Golgi paired stacks. In both models, one stack of the pair is drawn in a warm color (yellow, orange, red, and pink), and the second stack in a cold color (purple, and light and dark blue). The ER is modeled in broken white and surrounds the paired stacks.

The models without the ER are presented in (H'), (H'') and (I'), (I'') at different angles. For more details, see Movies S4 and S5. The white arrow in (H'') points to the middle cisterna (light blue) that is very close to the adjacent stack, perhaps connected. The double arrow in (I'') points to a cisterna (purple) that is shared by both stacks in the pair. The distance between the two stacks is less than 70 nm.

The scale bars represent 200 nm.

and Abi-V5/GFP (Figures 7B and 7C) were found to partially localize at the periphery and between the paired Golgi stacks.

F-Actin Depolymerization and Abi/Scar Depletion Mimic G2 Golgi Separation

To assess whether the Golgi doubling that we observed at G2 involves rearrangements in the F-actin cytoskeleton around the Golgi, we first compared the number of Golgi stacks in G1 and S/G2 cells treated with F-actin depolymerizing drugs. Our prediction is that if a change in F-actin dynamics underlies Golgi separation at G2, the actin-based mechanism that maintains the two Golgi stacks

together should be severed/modified in a G2-specific manner, and therefore become insensitive to CytoD and LatB treatment, preventing further Golgi splitting. In contrast, the paired Golgi in G1 cells should separate.

We used the number of centrosomes to distinguish G1 from S/G2 cells in a nonsynchronized (Figures 1A–1F) or a G2 enriched cell population (using the topoisomerase II inhibitor doxorubicin, which induces a strong delay in exiting G2; van Vugt et al., 2004). LatB-treated S/G2 cells exhibited a similar number of Golgi spots as DMSO-treated S/G2 cells (Figure 7D; Table S1), whereas G1 cells exhibited a significant increase in their Golgi stack number, as reported for nonstaged cells (Table S1).

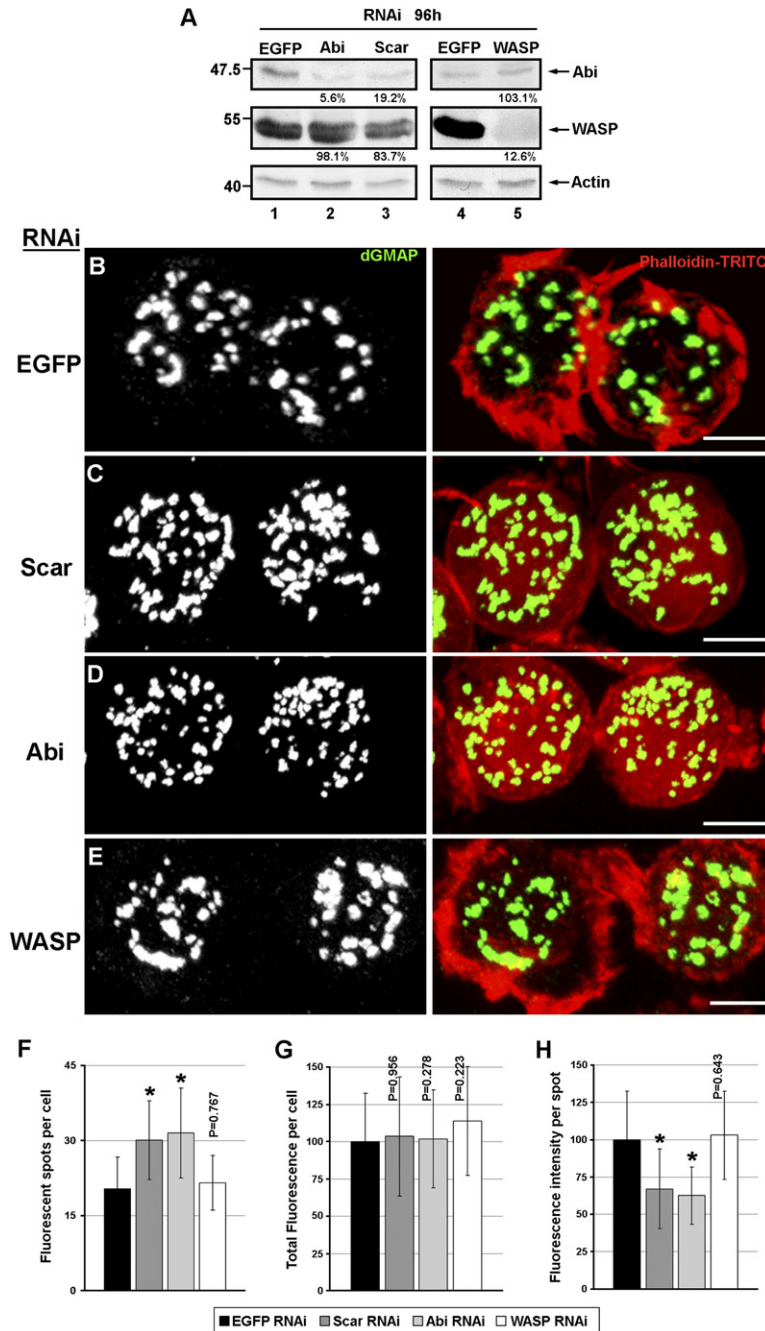


Figure 6. RNAi Depletion of Scar and Abi, but Not WASP, Leads to a Doubling in the Number of tER-Golgi Units

(A) Western blotting of S2 cell extract after 96 hr incubation with dsRNAs to EGFP (lanes 1 and 4), Abi (lane 2), Scar (lane 3), and WASP (lane 5) using anti-Abi, anti-WASP, and anti-actin antibodies. The percentage indicates the amount of protein left after depletion when compared to EGFP and normalized to actin.

(B–E) IF visualization of the Golgi (dGMAP) and the actin network (phalloidin) in S2 cells that are mock- (EGFP, [B]), Scar- (C), Abi- (D), and WASP- (E) depleted.

(F–H) ImageJ quantification of the number of fluorescent Golgi spots per cell (F), total fluorescence per cell (G), and the average fluorescence intensity per spot (H). Error bars represent standard deviation (SD), and asterisks indicate conditions under which a statistical significant change ($p \leq 0.001$) is calculated.

The scale bars represent 5 μm .

Next, we examined whether the G2 separation of paired Golgi stacks is regulated by Abi and Scar. Again, the prediction was that if this takes place specifically at G2 by modulation of their activity, then Abi/Scar-depleted cells (in which the Golgi has already been separated) should exhibit a similar number of tER-Golgi units at G1 and S/G2. This was exactly what we observed. Abi/Scar-depleted G1 cells had a comparable number of Golgi spots as their S/G2 counterparts (Figures 7E and 7F; Table S1). As a control, WASP-depleted cells exhibited an S/G2 increase in their Golgi number in a similar fashion as mock-depleted cells (Figures 7E and 7F).

Last, we reasoned that the separation of the paired tER-Golgi units at G2, prior to their mitotic dispersion, might be essential for mitotic entry. To test this, we over-expressed Abi, which prevented the splitting of the Golgi stacks at G2 (the number of Golgi spots was 15.9 ± 4.4 , matching this in G1 cells; Figure 7G). Strikingly, the mitotic index of the transfected cells dropped to 0.4%, an 82% decrease when compared to 2.5% in nontransfected cells (Figure 7H).

Overall, these results show that during G1/S, the Golgi complex is made up of two stacks maintained in a pair by Abi/Scar-mediated F-actin polymerization at this

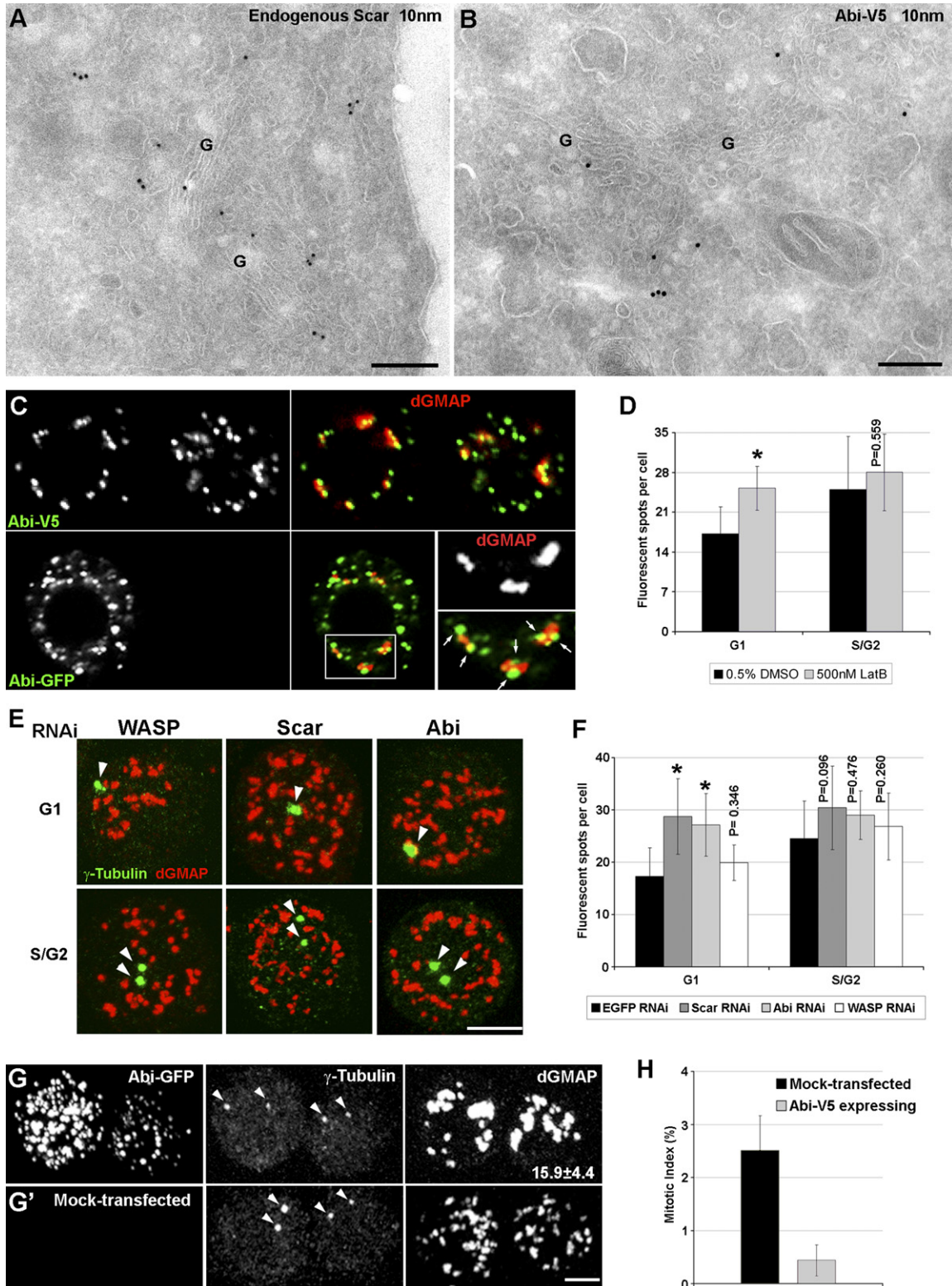


Figure 7. The Golgi Is Separated at G2 through Changes in F-Actin Dynamics by Modulation of Abi and Scar

(A and B) Localization of endogenous Scar and Abi-V5 (3 hr expression) by IEM on and around paired Golgi stacks. G, Golgi stacks. (C) Single confocal section of Abi-V5 and Abi-GFP immunolocalization in double labeling with the Golgi marker dGMAP. Note in the enlarged inset that Abi (small arrows) often localizes in the middle and at the periphery of the Golgi spots. (D) ImageJ quantification of the number of fluorescent Golgi spots in G1 and S/G2 S2 cells after mock and LatB treatment and labeling for the Golgi and the centrosomes (as in Figure 1A).

location. This mechanism is severed at G2 to lead to the Golgi stack separation that is required for cell entry and progression in mitosis.

DISCUSSION

Golgi: A Paired Organelle Held by F-Actin

We show here that the Golgi is a preduplicated organelle throughout a large part of the cell cycle, and that each Golgi comprises not one, but a pair of stacks held together through an F-actin-based mechanism. We show that a near-doubling in the Golgi number occurs through the separation of the two stacks both at G2 (see below) and upon F-actin depolymerization. Such a paired organelle has been proposed to exist in *Toxoplasma* (Pelletier et al., 2002), and this arrangement is reminiscent of the centriole, another paired organelle that plays a crucial role during the cell cycle.

The two stacks could be physically linked without displaying membrane continuity or being interconnected, for instance through intercisternal tubular connections, either permanent or transient. Tubules connecting cisternae of adjacent stacks are involved in the formation of the Golgi ribbon in mammalian cells (Ladinsky et al., 1999) and, recently, GM130 and GRASP65 have been proposed to be required for their integrity (Puthenveedu et al., 2006). However, the putative tubules connecting the two stacks in the pair would have different molecular requirements, at least in *Drosophila*, as depletion of dGM130 or dGRASP does not lead to their separation (Kondylis and Rabouille, 2003; Kondylis et al., 2005).

F-actin could provide a physical link holding the paired Golgi stacks together, or it could help in the formation/maintenance of intercisternal tubules. In addition, short actin filaments have been proposed to link spectrin mosaics leading to the formation of a skeleton that surrounds the Golgi complex (De Matteis and Morrow, 2000). One of its functions could be to hold the two Golgi stacks close enough to allow the formation and fusion of the tubules. It could also surround the tubules themselves, thus providing membrane stability. The localization of Abi and Scar at the periphery of the tER-Golgi units and between the two stacks in a pair is consistent with both proposed functions. Our tomography studies so far have not revealed clear membrane continuities between Golgi cisternae, though we have found examples of a tubular network which is shared by the paired stacks.

tER sites behave similarly to the Golgi, as they also separate at G2 and upon F-actin depolymerization. Because little is known about the mechanism regulating the biogen-

esis of tER sites, it is difficult here to envisage how the two parts could be held together. The spectrin-actin mesh described above could be common to Golgi and tER sites, and Golgi and tER site scission could be achieved in a synchronized fashion. Alternatively, either of these organelles could split first and lead to the scission of the other, perhaps by providing positional information. Recently, the centrosome component centrin 2 that is also localized to tER sites in *Trypanosoma* has been shown to give such positioning information (He et al., 2005). A more in-depth study combining immunogold labeling and 3D tomography would be required to elucidate such fine details of tER-Golgi structural organization.

Molecular Regulation of Golgi Stack Pairing: Scar and Abi

Drosophila Rho1 is unlikely to have a role in holding the two Golgi stacks together. The overexpression of the Rho1 constitutively inactive mutant or treatment of S2 cells with ROCK or myosin light chain inhibitors (Y27632 and blebbistatin; data not shown) did not affect the Golgi number. Cdc42 is also unlikely to participate as the depletion of its downstream effector WASP did not lead to Golgi separation, although the overexpression of the Cdc42^{T17N} dominant negative did. However, this effect could be due to nonspecific sequestration of the guanine nucleotide exchange factor involved in maintaining the paired Golgi stacks and may be shared with other small GTPases.

Interestingly, our results are consistent with a role for Rac GTPases in *Drosophila* Golgi architecture. Expression of the constitutively inactive form of Rac1 led to a near-doubling in the Golgi number, and depletion of Scar/WAVE or Abi, which are regulated by Rac GTPases, led to a similar phenotype. The identical results we obtained in Scar and Abi RNAi suggest that this well-established Scar/WAVE pentameric complex is involved in holding the paired Golgi stacks together by promoting F-actin polymerization. These data indicate that the Rac signaling pathway is involved. However, the Scar/Abi complex has recently been shown to also stimulate Arp2/3 and F-actin polymerization independently of Rac (Innocenti et al., 2004). This would need to be investigated further.

The Paired Golgi Stack Is Separated at G2 by Modulation of Abi and Scar

We show here that the separation of the paired Golgi stacks occurs at G2, prior to mitosis. A similar phenomenon has already been reported during cell division in *Toxoplasma gondii* (Pelletier et al., 2002), where a single Golgi stack grows as a duplicated organelle and is separated as

(E and F) Representative examples and ImageJ quantitation of the number of fluorescent Golgi spots in G1 and S/G2 cells after mock, Abi, Scar, and WASP depletion (F) and labeling for the Golgi and the centrosomes (E). (G and G') Visualization of the Golgi (dGMAP) in S/G2 cells (two centrosomes marked by γ -tubulin) in which Abi-GFP is overexpressed for 24 hr. Note that the number of Golgi spots (15.9 ± 4.4) is lower than in mock-transfected S/G2 cells (G'). (H) The mitotic index of Abi-GFP-transfected cells drops by 82% compared to mock-transfected cells. Arrowheads point to centrosomes. Error bars represent standard deviation (SD), and asterisks indicate conditions under which a statistical significant change ($p \leq 0.001$) is calculated. The scale bars represent 5 μ m.

the cell divides. However, the mechanism underlying this separation is not known.

The Golgi doubling in number at G2 phase resembles many aspects of this observed upon F-actin depolymerization. In both cases, a similar increase in Golgi number and decrease in their size are observed. Furthermore, we have shown that it is the modulation of the F-actin cytoskeleton and the activity of Abi/Scar at G2 that lead to Golgi stack separation. First, we found that both Scar and Abi localized to the Golgi, strongly arguing for having a role in actin remodeling around this organelle. Second, the Golgi stacks in G2 cells remain insensitive to F-actin depolymerization. Third, cells depleted of Abi and Scar that exhibit separated Golgi stacks do not split them further at G2. Fourth, the overexpression of Abi prevents Golgi separation at G2. This strongly suggests that the F-actin/Abi/Scar-mediated link of the two stacks has been severed in a G2-specific manner, perhaps by kinases such as Polo (Barr et al., 2004).

Because tER sites and the Golgi apparatus ultimately disperse later in mitosis, both in mammalian (Shorter and Warren, 2002; Stephens, 2003) and *Drosophila* S2 cells (Stanley et al., 1997; Figure S1), the Golgi stack separation prior to dispersion might be part of the proposed Golgi G2/M checkpoint. Indeed, reagents that interfere with the GRASP65/55 phosphorylation by Polo and ERK/MEK, respectively, arrest or delay the cell cycle at the G2/M transition (Sutterlin et al., 2002; Preisinger et al., 2005; Feinstein and Linstedt, 2007). Here we show that blocking Golgi separation at G2 by overexpressing Abi also prevents S2 cells from entering mitosis. This strengthens the relationship between Golgi organization and mitotic entry, although we cannot formally exclude that the mitotic block we observe is partly due to additional effects of Abi overexpression, for instance at the plasma membrane.

We propose that at G2, the paired stacks are separated along with the adjacent tER sites. As the cell enters mitosis, the Golgi membrane and the tER sites disperse, and are segregated into the two daughter cells, where the tER-Golgi units are rebuilt. The Golgi could be rebuilt as a very small paired stack in close association with Scar, Abi, and F-actin, or as a single stack that will duplicate by a mechanism that still needs to be unraveled. As G1 cells are all sensitive to F-actin depolymerization, this suggests that the formation of the paired Golgi stack starts just after the exit from mitosis and persists until S phase, when the Golgi seems to grow significantly (Figure S7). A more detailed understanding will come from EM study of S and G2 cells.

One of the remaining questions regards the impact of the Abi/Scar role on Golgi organization during development. Using Scar/WAVE, Abi, Kette, and Sra-1 mutants, as well as transgenic flies carrying inducible RNAi constructs (Bogdan et al., 2005), it will be possible to assess whether any of the observed phenotypes (defects in oogenesis, cell and organ morphology, neuroanatomical malformations, and failure in cell migration; for a review, see Stradal et al., 2004) is in part due to defects in Golgi organization.

EXPERIMENTAL PROCEDURES

Cells

Wild-type and Delta S2 cells, as well as flat S2R⁺ cells (gift from Sean Munro, Cambridge, UK), were grown as described (Kondylis and Rabouille, 2003). HeLa cells stably expressing GalNAcT2-GFP (gift from Tommy Nilsson, Göteborg, Sweden) were cultured as previously described (Storrie et al., 1998) in the presence of 400 μ g/ml G-418 sulfate to maintain the selection.

Identification of Cell-Cycle Phases in S2 Cells

Cells in G1 phase were characterized by their small size (<10 μ m in diameter) and exhibited a single centrosome. S/G2 phase cells were larger (≥ 10 μ m in diameter) and contained two centrosomes found in close proximity. The distinguishing feature between S and G2 cells was the BrdU-positive staining of the former. The different mitotic stages were identified by looking at α -tubulin, DAPI, and phosphohistone H3 staining. The mitotic index was estimated as the percentage of PH3-positive cells or cells with condensed chromosomes (visualized by DAPI staining) over the total cells counted. In all quantitative analyses, multinucleated cells or cells with abnormally bright, large, or fragmented DAPI staining were not taken into account.

BrdU Incorporation and Labeling

Cells were incubated for 1 hr with 20 μ M BrdU (Sigma) and fixed with 4% paraformaldehyde in PBS. Fixed cells were treated with 1% periodic acid at 60°C for 30 min, rinsed with tap water and dH₂O, and blocked with 5% BSA in PBS for 10 min. Subsequently, the cells were processed for immunofluorescence (Kondylis and Rabouille, 2003).

Cloning

The full-length Fringe and Abi coding sequences were amplified by PCR from clone SADFGM1-Fringe (gift from Sean Munro) and LD37010, respectively. Primers were used to introduce EcoRI/XhoI (Fringe) and EcoRI/NotI (Abi) restriction sites. Fringe and Abi were C-terminally tagged with EGFP or V5.

Transient Transfections

Transient transfections have been described in Kondylis et al. (2005). The metallothionein promoter allowed a tight and short induction of Fringe-GFP (3 hr with 1 mM CuSO₄) followed by a chase of 2 hr in the presence of 100 μ g/ml cycloheximide to block protein synthesis and allow the marker to specifically and exclusively localize to the Golgi stacks (Figures 3A and 3B). Abi was induced for 3 or 24 hr.

Drug Treatments

F-actin depolymerization in S2 cells was performed by incubating the cells with CytoD or LatB (final concentration 20 μ M and 500 nM, respectively) for up to 2 hr. Control cells were incubated with 0.5%–1% DMSO. BFA treatment was performed at the final concentration of 20 μ M for at least 30 min. Doxorubicin (Sigma) was added to the culture medium at a final concentration of 1 μ M for 1 hr, washed away thoroughly, and the cells were incubated for 16 hr to enrich the population of G2 cells. All incubations were carried out at 27°C. GalNAcT2-GFP-expressing HeLa cells were first treated with 10 μ g/ml nocodazole for 4 hr, followed by the addition of 500 nM LatB in the continuous presence of nocodazole.

RNA Interference

Double-stranded RNA (dsRNA) for WASP, Scar, and Abi were synthesized using specific PCR fragments cloned in the pLitmus28/38i vector kindly provided by Christian Klämbt (Munster, Germany; Bogdan et al., 2005). String/Cdc25 dsRNA was prepared from T7-flanked PCR fragments corresponding to nucleotides 6–613 of its coding sequence. The RNAi experiments were performed as in Kondylis and Rabouille (2003).

Antibodies

Antibodies raised against dSec23p, d120kd, dCOG3, p24 δ 1 (p23), GFP, and Delta (C594.9B) have been characterized before (Kondylis and Rabouille, 2003; Kondylis et al., 2005). A polyclonal antibody recognizing dGMAP was used to mark the Golgi membranes (Friggeri-Grelin et al., 2006). 20H5 is a monoclonal antibody raised in *Chlamydomonas reinhardtii* crossreacting with centrins from different species (Sanders and Salisbury, 1994). Monoclonal antibodies to α -tubulin (GTU-88), β -actin (AC15), and γ -tubulin (B5-1-2) were from Sigma, and anti-V5 was from Invitrogen. Rat anti-BrdU antibody (clone BU1/75 [ICR1], Oxford Biotechnology) and rabbit polyclonal anti-phosphohistone H3 (serine10; Upstate Biotechnology) were used to mark cells in S phase and mitosis, respectively. Anti-Scar (gift from Jennifer Zallen, New York) and anti-WASP (gift from Assel Biyasheva, Chicago) antibodies have been characterized in Zallen et al. (2002) and Biyasheva et al. (2004). Anti-Abi antibody (gift from Christian Klämbt) is described in Bogdan et al. (2005). Phalloidin-TRITC (Sigma) was used to detect F-actin.

Immunofluorescence Imaging and Analysis

S2 cells were fixed and processed for immunofluorescence (Kondylis and Rabouille, 2003). Images were acquired using a Leica TCS-NT or Zeiss LSM-510 confocal microscope, keeping the same acquisition settings for the different conditions within each experiment. Twenty-five to thirty optical sections spaced at 0.4 μ m were usually necessary to span the whole cell and capture its entire volume. Except for Figure 7C, the 2D projection is presented in the figures.

Manual Quantification

On a pilot quantification, the objects on 30 selected cells (DMSO- and LatB-treated cells) were manually traced throughout the stack on individual confocal sections and their number was recorded. The number of fluorescent spots was also counted on 2D projections of the same cells built from the individual confocal sections. Comparison between the two methods showed that the 2D projection resulted in underestimation of the number of fluorescent spots per cell by one to two spots, mostly due to the optical merging of spots belonging to different sections. All subsequent quantifications were performed on 2D projected images using this number as a correction factor.

ImageJ Quantification

Using ImageJ software (Version 1.34; <http://rsb.info.nih.gov/ij/>), the number of fluorescent objects was counted after applying a fixed threshold on projected pictures, excluding objects with size less than 2–3 pixels. The total fluorescence per cell and the average fluorescence per spot were estimated using the “analyze particles” function, and were normalized to control (set at 100%). Typically, each calculated average derives from two or three independent experiments per condition analyzing at least 30 cells per experiment (unless otherwise stated). The statistical significance of all data obtained was assessed by two-tailed unpaired Student's t tests. p values equal or lower than 0.001 were considered significant and are marked by an asterisk, whereas p values higher than 0.001 are indicated.

Time-Lapse Confocal Microscopy

S2 cells transiently transfected with Fringe-GFP and GalNAcT2-GFP HeLa cells were grown on 25 mm uncoated or concanavalin A-coated (Sigma) coverslips. For live cell imaging, the cells were transferred to a humidified culture chamber attached to a Zeiss LSM 510 confocal microscope and adjusted at 27°C for S2 cells or 37°C/5% CO₂ for HeLa cells. Images were captured using a 63 \times 1.4 NA Plan-Apo objective (Zeiss) starting 5–10 min after the addition of F-actin depolymerizing drugs to the medium and up to 30 min. For each time point, a stack of four to ten optical sections spaced \sim 0.4 μ m apart was collected. Scan times for a single optical section were approximately 1 s and stacks of optical sections were collected every 10–30 s. Each stack of optical sections was then average projected and the projected images were multiplied by an appropriate enhancement factor. Adobe Photoshop 8.0 was used to crop the merged images, increase the image size for easier viewing, and compress the images into a JPEG

format. The processed projections were converted to movies using ImageJ. Golgi splitting events seen in projected images were verified by tracking the fluorescent objects on individual confocal sections.

(Immuno)Electron Microscopy and Stereological Analysis

S2 cells were fixed and processed for electron microscopy (Kondylis and Rabouille, 2003; Kondylis et al., 2005). Using micrographs depicting entire cell profiles from ultrathin plastic sections of mock-, CytoD-, and LatB-treated S2 cells (final magnification 14,000–20,000), the boundaries of the tER-Golgi units were drawn. Their total surface (St) and the surface of individual tER-Golgi units (Si) were estimated by point hit using a grid of 2.5 μ m, whereas the surface of the cytoplasm (including all organelles except the nucleus) (Scyt) was estimated using a grid of 1 cm. The total surface density of tER-Golgi units and the surface density of individual tER-Golgi units were calculated as St/Scyt and Si/Scyt, respectively. The surface density of the nucleus was also calculated in cell profiles under all conditions and was found unchanged. Twenty cell profiles per condition were used.

The percentage of paired tER-Golgi units and the number of tER-Golgi units per cell section were estimated by examination under the microscope of 100 cells per condition. A pair is defined by the rim of one cisterna in one stack being less than 70 nm away from the rim of the closest cisterna in the second stack. A paired organelle was counted as two (Figure 5E). Student's t tests were performed as mentioned above.

Three-Dimensional Electron Tomography

The samples were processed for electron tomography as described by Zeuschner et al. (2006). Briefly, three consecutive thick (250 nm) sections of chemically (Karnovsky) fixed, epon-embedded wild-type S2 cells were poststained and examined under a Tecnai 20 LaB6 transmission electron microscope (FEI Company, The Netherlands). Golgi areas of interest were captured in dual-axis tilt series from -60° to $+60^\circ$ with 1° increments at a magnification of 5000. In the program package IMOD (<http://bio3d.colorado.edu>), tilt series were aligned and the three serial sections were joined to form a 750 nm thick stack. Parts of this tomogram are displayed in Figure 5H (500 nm) and Figure 5I (250 nm). Every virtual slice was viewed and analyzed, but only every second one was drawn by tracing the membrane manually. Similar tomograms were obtained with high-pressure-frozen cells, but slight cell ice damage prevented complete modeling (data not shown).

Supplemental Data

Supplemental Data include seven figures, one table, and five movies and are available at <http://www.developmentalcell.com/cgi/content/full/12/6/901/DC1/>.

ACKNOWLEDGMENTS

We thank Tommy Nilsson, Sean Munro, Christian Klämbt, Jennifer Zallen, Assel Biyasheva, Jeffrey Salisbury, and Rene Medema for gifts of reagents; Despina Xanthakis for help in cloning and IEM; Willie Geert (Dept. of Molecular Cell Biology, Utrecht University) for the use of the Tecnai; and Fulvio Reggiori and Sean Munro for critically reading and editing the manuscript. V.K. is supported by a ZonMw grant from the Nederlandse Organisatie voor Wetenschappelijk Onderzoek (NWO, 912-04-009) and by a Horizon Programme from National Regie-Organ Genomics (050-71-029), B.H. by an ASPASIA grant (NWO, 015-001-129), and H.E.v.N.t.P. by an ALW grant (NWO, 813.08.001).

Received: June 28, 2006

Revised: February 2, 2007

Accepted: March 9, 2007

Published: June 4, 2007

REFERENCES

- Altan-Bonnet, N., Sourgat, R., Liu, W., Snapp, E.L., Ward, T., and Lippincott-Schwartz, J. (2006). Golgi inheritance in mammalian cells is mediated through ER export activities. *Mol. Biol. Cell* **17**, 990–1005.
- Barr, F.A., Sillje, H.H., and Nigg, E.A. (2004). Polo-like kinases and the orchestration of cell division. *Nat. Rev. Mol. Cell Biol.* **5**, 429–440.
- Bevis, B.J., Hammond, A.T., Reinke, C.A., and Glick, B.S. (2002). De novo formation of transitional ER sites and Golgi structures in *Pichia pastoris*. *Nat. Cell Biol.* **4**, 750–756.
- Biyasheva, A., Svitkina, T., Kunda, P., Baum, B., and Borisy, G. (2004). Cascade pathway of filopodia formation downstream of SCAR. *J. Cell Sci.* **117**, 837–848.
- Bogdan, S., Stephan, R., Lobke, C., Mertens, A., and Klambt, C. (2005). Abi activates WASP to promote sensory organ development. *Nat. Cell Biol.* **7**, 977–984.
- Camera, P., da Silva, J.S., Griffiths, G., Giuffrida, M.G., Ferrara, L., Schubert, V., Imarisio, S., Silengo, L., Dotti, C.G., and Di Cunto, F. (2003). Citron-N is a neuronal Rho-associated protein involved in Golgi organization through actin cytoskeleton regulation. *Nat. Cell Biol.* **5**, 1071–1078.
- De Matteis, M.A., and Morrow, J.S. (2000). Spectrin tethers and mesh in the biosynthetic pathway. *J. Cell Sci.* **113**, 2331–2343.
- Dubois, T., Paleotti, O., Mironov, A.A., Fraissier, V., Stradal, T.E., De Matteis, M.A., Franco, M., and Chavrier, P. (2005). Golgi-localized GAP for Cdc42 functions downstream of ARF1 to control Arp2/3 complex and F-actin dynamics. *Nat. Cell Biol.* **7**, 353–364.
- Egea, G., Lazaro-Diequez, F., and Vilella, M. (2006). Actin dynamics at the Golgi complex in mammalian cells. *Curr. Opin. Cell Biol.* **18**, 168–178.
- Engqvist-Goldstein, A.E., and Drubin, D.G. (2003). Actin assembly and endocytosis: from yeast to mammals. *Annu. Rev. Cell Dev. Biol.* **19**, 287–332.
- Feig, L.A. (1999). Tools of the trade: use of dominant-inhibitory mutants of Ras-family GTPases. *Nat. Cell Biol.* **1**, E25–E27.
- Feinstein, T.N., and Linstedt, A.D. (2007). Mitogen-activated protein kinase 1-dependent Golgi unlinking occurs in G2 phase and promotes the G2/M cell cycle transition. *Mol. Biol. Cell* **18**, 594–604.
- Friggi-Grelin, F., Rabouille, C., and Therond, P. (2006). The *cis*-Golgi *Drosophila* GMAP has a role in anterograde transport and Golgi organization in vivo, similar to its mammalian orthologue in tissue cultured cells. *Eur. J. Cell Biol.* **85**, 1155–1166.
- Hammond, A.T., and Glick, B.S. (2000). Dynamics of transitional endoplasmic reticulum sites in vertebrate cells. *Mol. Biol. Cell* **11**, 3013–3030.
- He, C.Y., Pypaert, M., and Warren, G. (2005). Golgi duplication in *Trypanosoma brucei* requires Centrin2. *Science* **310**, 1196–1198.
- Herspers, B.H.A., and Rabouille, C. (2004). mRNA localization and ER-based protein sorting mechanisms dictate the use of tER-Golgi units involved in gurken transport in *Drosophila* oocytes. *Mol. Biol. Cell* **15**, 5306–5317.
- Innocenti, M., Zucconi, A., Disanza, A., Frittoli, E., Areces, L.B., Steffen, A., Stradal, T.E., Di Fiore, P.P., Carlier, M.F., and Scita, G. (2004). Abi1 is essential for the formation and activation of a WAVE2 signalling complex. *Nat. Cell Biol.* **6**, 319–327.
- Jaffe, A.B., and Hall, A. (2005). Rho GTPases: biochemistry and biology. *Annu. Rev. Cell Dev. Biol.* **21**, 247–269.
- Kondylis, V., and Rabouille, C. (2003). A novel role for dp115 in the organization of tER sites in *Drosophila*. *J. Cell Biol.* **162**, 185–198.
- Kondylis, V., Spoorendonk, K.M., and Rabouille, C. (2005). dGRASP localization and function in the early exocytic pathway in *Drosophila* S2 cells. *Mol. Biol. Cell* **16**, 4061–4072.
- Kunda, P., Craig, G., Dominguez, V., and Baum, B. (2003). Abi, Sra1, and Kette control the stability and localization of SCAR/WAVE to regulate the formation of actin-based protrusions. *Curr. Biol.* **13**, 1867–1875.
- Ladinsky, M.S., Mastronarde, D.N., McIntosh, J.R., Howell, K.E., and Staehelin, L.A. (1999). Golgi structure in three dimensions: functional insights from the normal rat kidney cell. *J. Cell Biol.* **144**, 1135–1149.
- Lazaro-Diequez, F., Jimenez, N., Barth, H., Koster, A.J., Renaud-Piqueras, J., Llopis, J.L., Burger, K.N., and Egea, G. (2006). Actin filaments are involved in the maintenance of Golgi cisternae morphology and intra-Golgi pH. *Cell Motil. Cytoskeleton* **63**, 778–791.
- Lippincott-Schwartz, J., Yuan, L.C., Bonifacino, J.S., and Klausner, R.D. (1989). Rapid redistribution of Golgi proteins into the ER in cells treated with brefeldin A: evidence for membrane cycling from Golgi to ER. *Cell* **56**, 801–813.
- Matas, O.B., Martinez-Menarguez, J.A., and Egea, G. (2004). Association of Cdc42/N-WASP/Arp2/3 signaling pathway with Golgi membranes. *Traffic* **5**, 838–846.
- Moshkin, Y.M., Mohrmann, L., van Ijcken, W.F., and Verrizzer, C.P. (2007). Functional differentiation of SWI/SNF remodelers in transcription and cell cycle control. *Mol. Cell Biol.* **27**, 651–661.
- Munro, S. (2002). More than one way to replicate the Golgi apparatus. *Nat. Cell Biol.* **4**, E223–E224.
- Munro, S., and Freeman, M. (2000). The notch signalling regulator fringe acts in the Golgi apparatus and requires the glycosyltransferase signature motif DXD. *Curr. Biol.* **10**, 813–820.
- Pecot, M.Y., and Malhotra, V. (2004). Golgi membranes remain segregated from the endoplasmic reticulum during mitosis in mammalian cells. *Cell* **116**, 99–107.
- Pelletier, L., Stern, C.A., Pypaert, M., Sheff, D., Ngô, H.M., Roper, N., He, C.Y., Hu, K., Toomre, D., Coppens, I., et al. (2002). Golgi biogenesis in *Toxoplasma gondii*. *Nature* **418**, 548–552.
- Polishchuk, R.S., Polishchuk, E.V., and Mironov, A.A. (1999). Coalescence of Golgi fragments in microtubule-deprived living cells. *Eur. J. Cell Biol.* **78**, 170–185.
- Preisinger, C., Komer, R., Wind, M., Lehmann, W.D., Kopajtich, R., and Barr, F.A. (2005). PIK1 docking to GRASP65 phosphorylated by Cdk1 suggests a mechanism for Golgi checkpoint signalling. *EMBO J.* **24**, 753–765.
- Puthenveedu, M.A., Bachert, C., Puri, S., Lanni, F., and Linstedt, A.D. (2006). GM130 and GRASP65-dependent lateral cisternal fusion allows uniform Golgi-enzyme distribution. *Nat. Cell Biol.* **8**, 238–248.
- Sanders, M.A., and Salisbury, J.L. (1994). Centrin plays an essential role in microtubule severing during flagellar excision in *Chlamydomonas reinhardtii*. *J. Cell Biol.* **124**, 795–805.
- Savvidou, E., Cobbe, N., Steffensen, S., Cotterill, S., and Heck, M.M. (2005). *Drosophila* CAP-D2 is required for condensin complex stability and resolution of sister chromatids. *J. Cell Sci.* **118**, 2529–2543.
- Shima, D.T., Haldar, K., Pepperkok, R., Watson, R., and Warren, G. (1997). Partitioning of the Golgi apparatus during mitosis in living HeLa cells. *J. Cell Biol.* **137**, 1211–1228.
- Shorter, J., and Warren, G. (2002). Golgi architecture and inheritance. *Annu. Rev. Cell Dev. Biol.* **18**, 379–420.
- Stanley, H., Botas, J., and Malhotra, V. (1997). The mechanism of Golgi segregation during mitosis is cell type-specific. *Proc. Natl. Acad. Sci. USA* **94**, 14467–14470.
- Stephens, D.J. (2003). De novo formation, fusion and fission of mammalian COPII-coated endoplasmic reticulum exit sites. *EMBO Rep.* **4**, 210–217.
- Storrie, B., White, J., Rottger, S., Stelzer, E.H., Sugauma, T., and Nilsson, T. (1998). Recycling of Golgi-resident glycosyltransferases through the ER reveals a novel pathway and provides an explanation for nocodazole-induced Golgi scattering. *J. Cell Biol.* **143**, 1505–1521.
- Stradal, T.E., Rottner, K., Disanza, A., Confalonieri, S., Innocenti, M., and Scita, G. (2004). Regulation of actin dynamics by WASP and WAVE family proteins. *Trends Cell Biol.* **14**, 303–311.

Sutterlin, C., Hsu, P., Mallabiabarrena, A., and Malhotra, V. (2002). Fragmentation and dispersal of the pericentriolar Golgi complex is required for entry into mitosis in mammalian cells. *Cell* 109, 359–369.

Thyberg, J., and Moskalewski, S. (1999). Role of microtubules in the organization of the Golgi complex. *Exp. Cell Res.* 246, 263–279.

Valderrama, F., Duran, J.M., Babia, T., Barth, H., Renau-Piqueras, J., and Egea, G. (2001). Actin microfilaments facilitate the retrograde transport from the Golgi complex to the endoplasmic reticulum in mammalian cells. *Traffic* 2, 717–726.

van Vugt, M.A., Bras, A., and Medema, R.H. (2004). Polo-like kinase-1 controls recovery from a G2 DNA damage-induced arrest in mammalian cells. *Mol. Cell* 15, 799–811.

Zallen, J.A., Cohen, Y., Hudson, A.M., Cooley, L., Wieschaus, E., and Schejter, E.D. (2002). SCAR is a primary regulator of Arp2/3-dependent morphological events in *Drosophila*. *J. Cell Biol.* 156, 689–701.

Zeuschner, D., Geerts, W.J., van Donselaar, E., Humbel, B.M., Slot, J.W., Koster, A.J., and Klumperman, J. (2006). Immuno-electron tomography of ER exit sites reveals the existence of free COPII-coated transport carriers. *Nat. Cell Biol.* 8, 377–383.